# PHOTOACOUSTIC STUDY ON THE OPTICAL PROPERTIES OF ALUMINIUM-DOPED CADMIUM SULPHIDE THIN FILMS

A. FERNÁNDEZ-PÉREZ[a*], M. G. SANDOVAL-PAZ[b], R. SAAVEDRA[b,c]
*aDepartamento de Física, Facultad de Ciencias, Universidad del Bío-Bío, Collao 1202, Casilla 5-C, Concepción, Chile.*
*bDepartamento de Física, Facultad de Ciencias Físicas y Matemáticas, Universidad de Concepción, Casilla 160-C, Concepción, Chile.*
*cCenter for Optics and Photonics, Universidad de Concepción, Casilla 4016, Concepción, Chile.*

Aluminium doped and undoped Cadmium Sulphide thin films (CdS:Al) were deposited on glass substrates using the chemical bath deposition technique, in an ammonia-free cadmium-sodium citrate system. Films were synthetized varying Al content and deposition times. The optical properties of the CdS:Al films were determined from photoacoustic and optical transmission spectroscopies. Structural and morphological properties were investigated by X-ray diffraction (XRD) and atomic force microscope (AFM). The increasing of Al in the reaction solution yields a smaller crystallite size and higher energy band gap, in the range 2.42 - 2.60 eV.

## 1. Introduction

Over the years, the optical and electrical properties of Cadmium Sulphide (CdS) have been the subject of intense research due to its wide variety of technological applications, such as opto-electronic devices [1] and thin film solar cells [2-5]. For thin film solar cells based on CdTe and Cu(InGa)Se$_2$ (CIGS) absorber layers, CdS is the most commonly used optical window material due to high optical transparency, wide band gap (2.42 eV), n-type conductivity and thickness of about 100 nm [3-5].

It is clear that an increase in the number of high energy photons that are absorbed by the absorber layer improves the blue response of the solar cell. In this sense, the band gap value of CdS is less than other materials such Zinc Sulphide (ZnS), which has a band gap value of 3.8 eV. Recent works on CIGS-based thin film solar cells, that separately use both CdS and ZnS as optical windows, show that the use of CdS as a buffer layer produces a better conversion efficiency than ZnS (19.9% v/s 18.5%) [5-7]. In this way, increasing the band gap of CdS, by means of the introduction of impurities on the film, without substantially changing its lattice structure, could lead to an improvement in the efficiency of thin film based solar cells, as shown in [8] for Boron-doped CdS thin films used as a window layer in a CdTe/CdS solar cell.

Currently, one of the most inexpensive and scalable methods to prepare CdS thin films is chemical bath deposition (CBD), which uses a controlled chemical reaction to grow thin films by precipitation. To achieve this, substrates are vertically immersed in an alkaline solution containing the chalcogenide source, the metal ion and a complexing agent. Several works on the deposition of CdS with this technique employ ammonia (NH$_3$) in the chemical bath as the complexing agent and hydroxide source [7,9], which is a highly toxic material. Regardless, previous works shows that good quality CdS thin films can be prepared by CBD without ammonia, using another complexing agents like sodium citrate [10], potassium nitrilotriacetate [11] and nitrilotriacetic acid [12].

---

* Corresponding author:arturofe@ubiobio.cl

In terms of the introduction of impurities in the films, the effect of doping agents on CdS thin films synthetized by CBD have different effects on their optical, electrical and structural properties [8,13-17]. In particular, authors report in [13,16] an increase in the bandgap of doped CdS films when crystallite size decreases.

The purpose of this work is to investigate the optical properties of CdS:Al thin films that were grown by CBD in an ammonia-free system. In this sense, we want to compare the results between photoacoustic spectroscopy (PAS) and optical transmission (OT) measurements. Additionally, we study the the effects of the doping agent on structural and morphological properties of the films by means of X-ray diffraction (XRD) and atomic force microscope (AFM), respectively.

## 2. Experimental

Several sets of CdS films were grown by chemical bath deposition (CBD) on glass substrates (25 mm $\times$ 75 mm $\times$ 1 mm) using bath solutions with different concentrations of Al and different deposition times. The recipe to prepare doped CdS films is described in [10], referred to as AF films, and is based on a mixture of the following reactants: Cadmium Chloride ($CdCl_2$ * $2,5H_2O$, 98%, Sigma-Aldrich) Sodium Citrate ($C_6H_5O_7Na_3$, 99%, Sigma-Aldrich) Potassium Hydroxide (KOH, 88%, J. T. Baker) Thiourea ($CS(NH_2)_2$, 99%, Sigma-Aldrich) and pH 10 borate buffer.

The doping was performed by adding aluminium chloride ($AlCl_3$ * $6H_2O$, 99%, Sigma-Aldrich) to the mixture, with different molar ratios in solution, R = [Al]/[Cd] (0.00, 0.01, 0.03, 0.05, 0.07, 0.10 and 0.15), where the initial concentration of Cd at 0.5 M remains constant. The glass substrates were previously rinsed with deionized water and dried at room temperature. The films were grown at a bath temperature of 70°C. A set of five samples was deposited for each R value by placing the substrates in the reaction beaker and then removing them subsequently from the solution after 60, 120, 180, 240 and 270 minutes, respectively.

The optical properties of the films were evaluated by using PAS and OT measurements. For PAS measurements, we use a conventional photoacoustic cell, where the sample is placed inside an airtight chamber and illuminated with modulated light through a window. The output from a 1 kW Xe arc lamp source, through a step-motor driven monochromator assembly, served as the light source. The output light beam was modulated with a mechanical chopper ($f$ = 10 Hz). Detection of the PAS signal was done by a commercial electret microphone and a preamplifier connected to a dual phase lock-in amplifier. The PA spectrum was recorded in the wavelength range of 350 - 700 nm. Black carbon powder was prepared to normalize the source dependence of the signal. Is important to note that PAS is not a conventional technique for determining the band gap of transparent thin films, and is used in the vast majority of cases to evaluate absorption of opaque samples. However, it has been used previously to calculate the band gap of semiconductors directly from their absorption spectrums [18-19].

For OT measurements, a fiber optic detection spectrophotometer setup was used. The light beam from a QTH UV-VIS source is transferred to an optical fiber and then focused on the films by a lens. Transmitted light is transferred to a mini-spectrophotometer (Ocean Optics, Model USB 4000) to obtain spectra in the wavelength range 400 - 900 nm.

Finally, in order to determine the structural properties of the films, X-ray diffraction measurements (XRD) was carried out using a Bruker Endeavor D4 unit (with 40 kV, 20 mA Cu-$K_\alpha$ radiation, $\lambda$ = 0.15406 nm). Additionally, surface morphology was examined by atomic force microscope (AFM) using a Nanosurf Naio model, in contact mode.

## 3. Results and discussions

The CdS:Al films obtained were yellowish, homogeneous, with good adherence to the substrate, and had an appreciable change in color for a high content of Al in solution (R=0.15) acquiring a light-bluish tone.

In order to study the optical properties of the samples, we perform two different spectroscopies on the films: PAS and OT. Then, we compare the results obtained, and the band gap calculated from the measured spectra, for different doping levels and deposition times.

To calculate the band gap from the PAS spectrum, we observe that CdS:Al films are thermally thin samples. The thermal diffusion coefficient of the sample is $a=((\pi f)/\beta)^{1/2}$, where $\beta$ is the film thermal diffusivity coefficient (0.15 cm$^2$/s for CdS) and $f$ is the chopper modulation frequency (10 Hz). In this case, they satisfy the relation $ta\square1$, where $t$ is the thickness of the films. For this reason, the PAS signal is proportional to the optical absorption coefficient $\alpha$ [20].

Next, we can calculate the band gap for each sample, using the following relation between the optical absorption coefficient $\alpha$ and the incident photon energy $h\nu$ as,

$$\alpha = K(h\nu - E_g)^{n/2} \qquad (1)$$

where $K$ is a constant, $E_g$ is the band gap, and $n$ is equal to 1 for direct band gap materials such as CdS [21,22]. The bandgap was determined by plotting $\alpha^2$ v/s $h\nu$ and then extrapolating the straight-line portion to the energy axis [12-14]. In this way, we can estimate the band gap energy ($E_g$) according to the model for allowed direct transitions (Eq. (1)) and the square of the PAS signal. In Fig. 1 we show the PAS spectrums of the samples grown for 120 minutes, with R=0.00, R=0.03, R=0.07 and R=0.10, and we observe strong absorption in the UV region with a decay in visible wavelengths. In Fig. 2, the square of the PAS signal vs photon energy (eV) is plotted for the same samples, to determine the band gap of the films. We found band gap values for these films in the range between 2.46 and 2.55 eV, and an enhancement of the band gap with increasing Al content. This result is similar to that found in [12], where the increment of strain in the films is related to a higher energy band gap. Also, previously reported results [12-14] show an inverse relation between crystallite size and energy band gap, as we also found in this case.
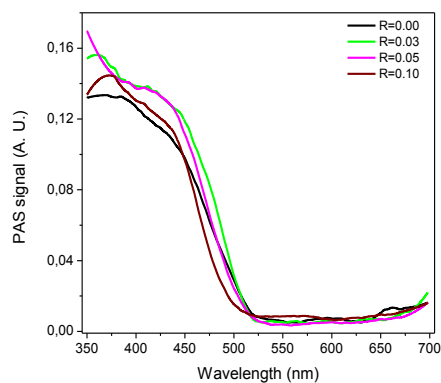


*Fig. 1. PAS spectrums for the CdS:Al films grown for 120 minutes, for different concentrations of Al.*
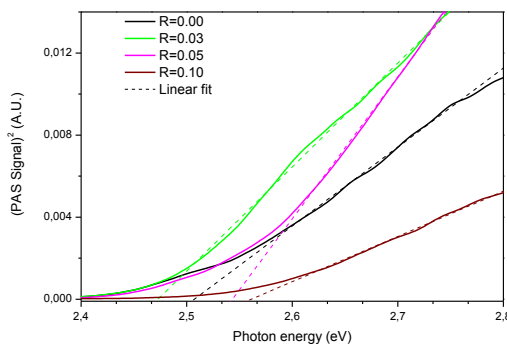


*Fig. 2: Square of the PAS signal vs photon energy, for CdS:Al films grown for 120 minutes, to obtain the band gap value for different concentrations of Al.*

The thickness of the CdS:Al films was obtained by analysing the optical transmittance spectrum. In Fig. 3, the transmittance spectra for some films grown for 120 minutes are shown, and a transmittance between 60% and 90% at visible wavelengths is observed. In order to estimate the film thickness, the transmittance spectra were fitted to a layer model by considering the samples to be constituted by an air/roughness/CdS:Al/glass system. The optical constants were represented by the SCI® model, which is a generalized version of the Lorentz harmonic oscillator expression, consistent with the Kramers-Kronig relations [23]. The optical constants of the roughness layer, defined as a mixture of CdS:Al and air in a proportion 50–50 %vol., were modeled by a Bruggeman's effective medium approximation [24]. The estimation of roughness value was given by the thickness of this layer and AFM measurements. From the fitting procedure, using the software *FilmWizard*[TM], the thickness and the roughness were obtained. The roughness values obtained were in a range between 3 and 6 nm for all samples, showing no clear trend with the Al content of the films and consistent with average surface roughness calculated from AFM micrographs, as we shall see later. Calculated thicknesses for the films with R values 0.03, 0.05, 0.10 and 0.15, grown by 60, 120, 180, 240 and 270 minutes, are shown in Table 1.
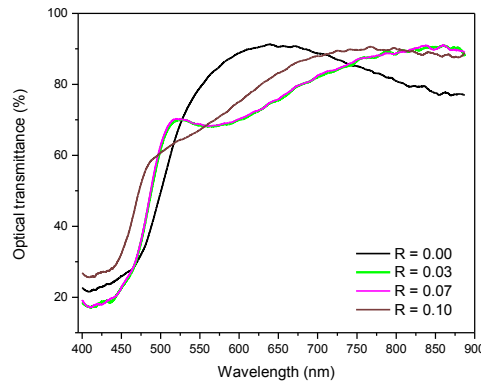


*Fig. 3: Optical transmittance spectrum of CdS:Al films grown for 120 minutes,*
*for different concentrations of Al*

*Table 1: Calculated film thickness (in nm) for different concentrations of Al and deposition times*

| Deposition Time | R=0.00 | R=0.03 | R=0.07 | R=0.10 |
|---|---|---|---|---|
| 60 min | 115.43 | 146.55 | 146.40 | 146.04 |
| 120 min | 140.66 | 165.53 | 176.29 | 161.11 |
| 180 min | 149.55 | 184.57 | 182.97 | 184.93 |
| 240 min | 143.03 | 208.95 | 226.97 | 197.08 |
| 270 min | 135.07 | 216.18 | 221.97 | 199.60 |

Additionally, we calculate the absorption coefficient $\alpha$ from the optical transmittance spectrum (T) using the relation,

$$\alpha = \frac{1}{t}\log\left(\frac{1}{T}\right) \qquad (2)$$

where $t$ is the film thickness. Then, we plot $\alpha^2$ v/s $h\nu$ and extrapolate the straight-line portion to the energy axis to obtain the band gap of the films, as we show in Fig. 4, for the films grown for 120 minutes.
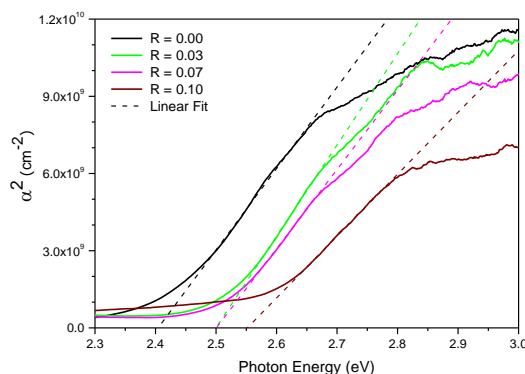
*Fig. 4. Square of the absorption coefficient vs photon energy, for CdS:Al films grown for 120 minutes, to obtain the band gap value for different concentrations of Al*

We observe a good agreement in the results obtained with both spectroscopic techniques, in terms of the calculated band gap, as we summarize in Fig. 5, for all R values and deposition times. An increase of the band gap of all the films is observed as Al content increases, and no significant change is observed for different deposition times. This is different to the previously reported result with Al-doped CdS films deposited by CBD [16], where the complexing agent used in the bath was ammonia, and films produced had thickness of about 110 nm, and band gap decreases as Al content increases. Here, we observe that the bandgap increases up to 2.60 eV, for samples grown for 120 minutes with R = 0.15, when film thickness is about 170 nm, and this is the highest band gap value that we obtained. We believe that band gap increment is related to the decreasing crystallite size, and the increase of the film microstresses [12].
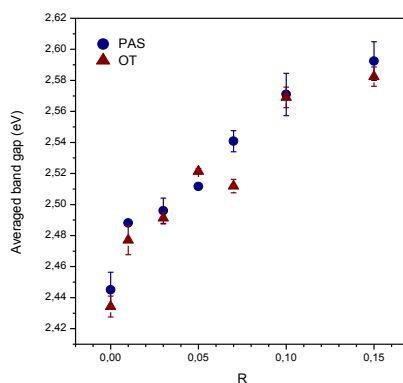


*Fig. 5. Comparison of the band gap of for CdS:Al films obtained with PAS and OT. Average value is calculated for all deposition times, for each R value, and error bars represent the standard deviation.*

To obtain these parameters, we investigate the structural properties of deposited CdS:Al thin films obtained by XRD. As an example, the diffraction patterns of the films grown for 120 minutes are shown in Fig. 6. The main peak occurs at $2\theta = 26.69°$, on average, for all samples. This maximum occurs in both the hexagonal and cubic phase, so it is not a good parameter to distinguish between them. However, if we analyze secondary peaks, which are much less intense than the main peak, we observe that some of them coincide with those that correspond to the hexagonal phase (wurtzite). In particular, we observe secondary peaks around $2\theta = 47.85°$ and $2\theta = 54.59°$ that correspond to (103) and (004) crystalline planes of the hexagonal phase and, therefore, the main peak matches with (002) planes of the wurtzite-type CdS.
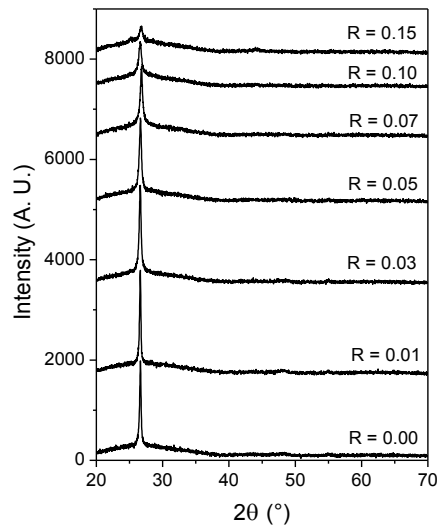
*Fig. 6: XRD pattern of the CdS:Al films grown for 120 minutes,
for different concentrations of Al*

Additionally, a decrease in the intensity of the main peak is observed when Al content increases. This result can be due to $Al^{3+}$ ions inducing dislocations and/or defects inside the lattice structure of CdS which causes a modification in the XRD pattern. The increase of FWHM of the main peak implies that $Al^{3+}$ ions induce lattice strain in the films. This can be deduced from the equation, $\left|\dfrac{\Delta d}{d}\right| = \dfrac{B}{2\tan\theta}$ , where B is the broadening (FWHM) due to fractional variations in the plane spacing $\left|\dfrac{\Delta d}{d}\right|$, and θ is the angle of the main peak position [18]. The value $\left|\dfrac{\Delta d}{d}\right|$ is a measure of the non-uniformity of the strain present in the lattice [25]. Also, we calculate the interplanar distance $d$ and crystallite size L, using Bragg's formula ($\lambda = 2d\sin\theta$) and Scherrer's formula (L $= 0.9\lambda/B\cos\theta$) respectively, with λ = 0.15406 nm. These crystallographic parameters are presented in Table 2.

*Table 2. Fractional variations in the plane spacing, interplanar distance and crystallite size,
related with (002) planes of CdS:Al thin films grown for 120 minutes*

| R | |Δd/d| | d (nm) | L (nm) |
|---|---|---|---|
| 0.00 | 0.00921 | 3.34365 | 35.58 |
| 0.01 | 0.00809 | 3.35583 | 40.54 |
| 0.03 | 0.01192 | 3.34982 | 27.50 |
| 0.05 | 0.01399 | 3.32884 | 23.42 |
| 0.07 | 0.01432 | 3.33476 | 22.82 |
| 0.10 | 0.01866 | 3.34973 | 17.57 |
| 0.15 | 0.02009 | 3.33945 | 16.26 |

Considering that the ionic radius of $Al^{3+}$ is 0.53 Å and is smaller than the ionic radius of $Cd^{2+}$ (0.95 Å) [26], the difference in the interplanar distance may be due to $Al^{3+}$ ions substitutionally replacing the $Cd^{2+}$ ions in the lattice, causing interplane distance decreases, which is observed when the doping concentration increases. However, if the ratio [Al]/[Cd] is greater than 0.05, $Al^{3+}$ ions are also incorporated into the interstitial states of the lattice, which implies that interplanar distance begins to increase. Crystallite size L ranges between 40 nm and 16 nm and we

observe a decrease of the crystallite size when the Al content in the bath solution increases, except for the lowest Al concentration, where we found a the biggest crystallite size.
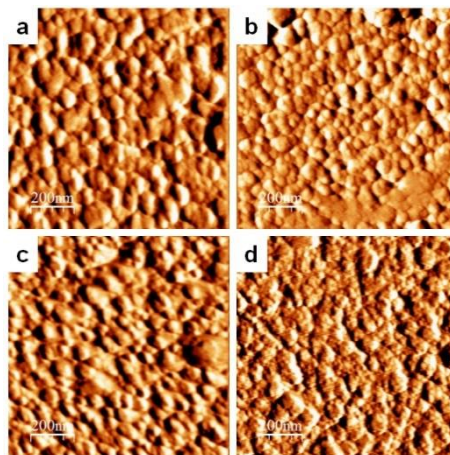


*Fig. 7. AFM micrographs of CdS:Al films grown for 120 minutes: (a) R = 0.00, (b) R = 0.03, (c) R = 0.07, (d) R = 0.10.*

Surface morphology of the films was analyzed by AFM in contact mode. In Fig. 7 we show the images obtained in an area of 1 x 1 $\mu m^2$. We observe, for different Al doping levels, a similar surface morphology, and for R=0.03 a dense layer of spherical grains. The average surface roughness, for the samples grown for 120 minutes with R=0.00, R=0.03, R=0.07 and R=0.10, is found to be 4.687 nm, 5.192 nm, 4.554 nm and 5.246 nm, respectively.

## 4. Conclusions

CdS:Al thin films were successfully deposited on glass substrates using an ammonia-free CBD process, where *in situ* Al-doping was performed. Photoacoustic and transmittance spectroscopies were performed on CdS:Al films, to obtain the optical absorption and transmission spectra, respectively. Then, the band gap of the films was calculated, both techniques yielding similar results. An increasing band gap value was observed with increasing Al content, compared to un-doped films, the resulting values range between 2.42 eV and 2.60 eV. No substantial change in the energy band gap was found for different deposition times. Film thickness was obtained by means of transmittance spectrum and specialized software, where the obtained values range between 146 and 256 nm, with increasing thickness when deposition time increases.

XRD measurements show a change in the intensity and the broadening of the main peak when Al doping is perfomed, indicating that the incorporation of $Al^{3+}$ ions slightly modifies the lattice structure of the CdS film. The average interplanar distance of CdS was modified with increasing Al-doping, due to dislocations produced by $Al^{3+}$ ions in the lattice, and the replacement of $Cd^{2+}$ ions in the lattice both substitutionally and interstitially. A decrease in the crystallite size was observed when we increase the amount of Al in the solution, from 40 nm to 16 nm. The nonuniformity of the strain present in the lattice increases with Al content, because crystallite size decreases and induces microstresses on CdS film. The enhancement of the band gap found in doped CdS films shows a direct relation with the increase in lattice strain and an inverse relation with crystallite size. AFM micrographs showed that the average surface roughness is in the range 4.5 - 5.2 nm.

Finally, the potential increment in the absorption of high energy photons, and the enhancement of the conversion efficiency of thin film solar cells based on CdTe and CIGS absorber layers, by using these CdS:Al films as a window layer, are now left as open questions.

514

**References**

[1] J. Zhao, J. A. Bardecker, A. M. Munro, M. S. Liu, Y. Niu, I. Ding, J. Luo, B. Chen, A. K.-Y. Jen, D. S. Ginger, Nanoletters **6**(3), 463 (2006).

[2] J. A. Bragagnolo, A. M. Barnett, J. E. Phillips, R. B. Hall, A. Rothwarf, J. D. Meakin, IEEE Transactions on Electron Devices **27**(4), 645 (1980).

[3] J. Han, C. Spanheimer, G. Haindl, G. Fu, V. Krishnakumar, J. Schaffner, C. Fan, K. Zhao, A. Klein, W. Jaegermann, Sol. Energy Mater. Sol. Cells **95**, 816 (2001).

[4] S. Shirakata, K. Ohkubo, Y. Ishii, T. Nakada, Sol. Energy Mater. Sol. Cells **93**, 988 (2009).

[5] I. Repins, B. Contreras, C. Egaas, J. Dehart, C. Scharf, B. Perkins, B. Noufi, Prog. Photovoltaics: Res. Appl. **16**, 235 (2008).

[6] R. N. Bhattacharya, M. A. Contreras, G. Teeter, Jpn. J. Appl. Phys. **43**, L1475 (2004).

[7] M. A. Contreras, M. J. Romero, B. To, F. Hasoon, R. Noufi, S. Ward, K. Ramanathan, Thin Solid Films **403–404**, 204 (2002).

[8] Jae-Hyeong Lee, Jun-Sin Yi, Kea-Joon Yang, Joon-Hoon Park, Ryum-Duk Oh, Thin Solid Films **431-432**, 344 (2003).

[9] H. Metin, R. Esen, J. Cryst. Growth **258**(1-2), 141 (2003).

[10] M. G. Sandoval-Paz, M. Sotelo-Lerma, A. Mendoza-Galvan, R. Ramírez-Bon, Thin Solid Films **515**, 3356 (2007).

[11] P. Nemec, I. Nemec, P. Nahalkova, Y. Nemcova, F. Trojanek, P.Maly, Thin Solid Films **403-404**, 9 (2002).

[12] H. Khallaf, I. O. Oladeji, L. Chow, Thin Solid Films **516**(18), 5967 (2008).

[13] H. Khallaf, G. Chai, O. Lupan, L. Chow, S. Park, A. Schulte, Appl. Surf. Sci. **255**, 4129 (2009).

[14] H. Khallaf, G. Chai, O. Lupan, L. Chow, H. Heinrich, S. Park, A. Schulte, Phys. Status Solidi A- Appl. Mat. **206**, 256 (2009).

[15] S. Mageswari, L. Dhivya, B. Palanivel, R. Murugan, J. Alloys Compounds **545**, 41 (2012).

[16] H. Khallaf, G. Chai, O. Lupan, L. Chow, S. Park, A. Schulte, J. Phys. D: Appl. Phys. **41**, 185304 (2008).

[17] C. D. Lokhande, S. H. Pawar, Solid State Commun. **44**, 1137 (1982).

[18] R. S. Ram, O. Prakash, A. N. Pandey, Pramana J. Phys. **28**, 293 (1987).

[19] M. L. Albor-Aguilera, M. A. González-Trujillo, A. Cruz-Orea, M. Tufiño-Velázquez, Thin Solid Films **517**, 2335 (2009).

[20] A. Rosencwaig, A. Gersho, J. Appl. Phys. **47**, 64 (1976).

[21] J. I. Pankove, Optical processes in semiconductors, Dover Publications Inc., New York, (1975).

[22] E. Rosencher, B. Vinter, Optoelectronics, Cambridge University Press, Cambridge (2004).

[23] E. Zawaideh, U.S. Patent No. 5889592 (1999).

[24] H. G. Tompkins, W. A. McGahan, Spectroscopic ellipsometry and reflectometry: A user's guide, John Wiley & Sons, Inc., New York (1999).

[25] B. D. Cullity, S. R. Stock, Elements of X-ray diffraction, Prentice Hall, New Jersey, (2001).

[26] R. D. Shannon, Acta Cryst. **A32**, 751 (1976).